

Prediction of optimum design variables for maximum heat transfer through a rectangular porous fin using particle swarm optimization[†]

Tuhin Deshamukhya, Dipankar Bhanja^{*}, Sujit Nath and Saheera Azmi Hazarika

Department of Mechanical Engineering, National Institute of Technology Silchar, Assam 788010, India

(Manuscript Received December 4, 2017; Revised May 13, 2018; Accepted May 22, 2018)

Abstract

The current study deals with the optimization of significant variables which govern the heat transfer from a porous fin in convective medium using particle swarm optimization (PSO). The temperature distribution of the fin is obtained analytically by a perturbation technique called homotopy perturbation method (HPM). To validate the temperature distribution obtained by HPM, finite difference method is employed. Next a significance analysis has been carried out to identify important variables that play a vital role in transferring heat from the porous fin. The set of variables thus obtained was then optimized by PSO to enhance the heat transfer rate. Reflective boundary condition is incorporated in the PSO to prevent particles from wandering in the infeasible region. The convergence plots of the variables show the effectiveness of PSO in solving non linear problems of this magnitude which are often encountered in the analysis of heat transfer through porous fins.

Keywords: Particle swarm optimization; Porous fin; Homotopy perturbation; Heat transfer

1. Introduction

Fins are an integral part of any device that generates heat during its working. The extensive research in this field has introduced the concept of porous fins for transferring better heat by improving the surface area of convection [1-3]. Advantages like material saving, weight minimization and increased surface area make these fins a good choice for a number of applications where weight, cost and space are major constraints.

Hatami et al. [4] studied analytically the heat transfer through porous fins made of Si_3N_4 and Al by considering temperature dependent heat generation. Again shape of the fin plays a major role in deciding the heat transfer capability of a fin. Thus, Bhanja and Kundu [5] determined analytically the temperature distribution and performance parameters of a constructal T shaped fin. A comparison between porous and solid straight fins of various profiles on the basis of heat transfer rate was done by Kundu et al. [6]. In another work by Bhanja et al. [7], the heat transfer rate through porous pin fins is found to be better than the solid fins of similar dimension and profile. In an analytical study involving the moving porous fins, Bhanja et al. [8] performed an optimization analysis by considering the effects of both convection and radiation.

Recently Hazarika et al. [9] performed an analytical study of a constructal T shaped porous fin under dehumidifying conditions. An effort has been made by Kundu and Bhanja [10] to study the optimum design analysis of porous fins considering a highly non-linear equation. The study was done for three different models. On the other hand, Das [11] proposed an inverse solution of a cylindrical porous fin exposed in both convective and radiative environment.

Recently, focus has been laid on optimizing the important parameters of heat transferring devices such as fins and heat exchangers [12-14]. The non linear equations obtained in these applications demand meta-heuristic algorithms to find the global optimized values of the parameters. Powerful nature inspired global optimization techniques such as genetic algorithm (GA), particle swarm optimization (PSO) and similar bio inspired stochastic algorithms have been used in a number of applications [15, 16] in the past few years. Recently a number of works have been performed on PSO related to the area of heat transfer [17, 18].

To the best of author's knowledge, there has not been any effort to study the multivariable optimization of porous fins using meta-heuristic algorithm. In the current work, particle swarm optimization (PSO), a swarm based meta-heuristic algorithm is selected to obtain the actual heat transfer rate by optimizing the important variables. The faster convergence ability and its derivative free nature make PSO a good choice for optimizing these kinds of problems. Therefore, the main

^{*}Corresponding author. Tel.: +91 9435175552, Fax.: +91 3842233797
E-mail address: dipankar.bhanja@gmail.com

[†]Recommended by Associate Editor Ji Hwan Jeong

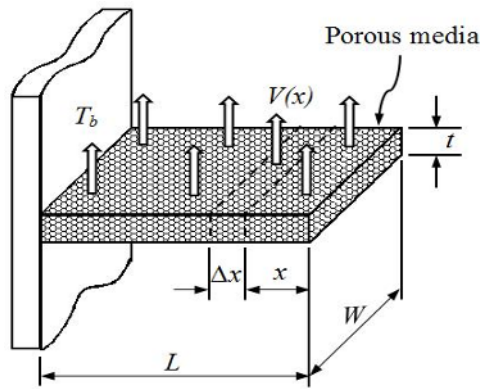


Fig. 1. Schematic diagram of a rectangular straight porous fin.

aim behind this work is to optimize the four key parameters in order to obtain the maximum heat transfer rate for a specified fin volume. Heat transfer rate is calculated by solving analytically the governing differential equation using homotopy perturbation method (HPM).

2. Problem definition

This study considers a rectangular porous fin as shown in Fig. 1. Being porous in nature, the fin allows fluid to penetrate through it and thus Darcy model is used to understand and analyze the interaction between the fluid and the porous medium in convective medium. In this work heat is transferred to the surrounding through the pores due to fluid penetration and the convective heat transfer through the solid part of the fin. Heat generation within the fin and radiation heat transfer is neglected and the temperature is considered to vary along one direction (x-axis) only. There is no contact resistance at the fin base and the wall. Porous medium is homogeneous, isotropic and saturated with a single phase fluid and the physical properties of solid as well as fluid are invariable except density of the fluid that may affect the buoyancy term where Boussinesq approximation is employed. The fin tip is considered to transfer heat through convection.

2.1 Governing equations

Applying energy balance and using Fourier’s law in a differential element of the fin, we obtain the governing differential equation for the porous fin as

$$\frac{d^2T}{dx^2} - \frac{2h(1-\phi)}{k_{eff}t}(T - T_a) - \frac{\dot{m}C_p}{k_{eff}Wt\Delta x}(T - T_a) = 0. \tag{1}$$

The mass flow rate, \dot{m} (in kg s^{-1}) of the fluid passing through fin pores is defined as

$$\dot{m} = \rho V W \Delta x. \tag{2}$$

ρ is the fluid density in kg m^{-3} and W in the fin width in m.

The fluid velocity V (in ms^{-1}) is estimated by Darcy’s law as [2]

$$V = gK\beta(T - T_a)/\gamma. \tag{3}$$

K is the permeability of the porous fin material in m^2 . The effective thermal conductivity (in $\text{W m}^{-1}\text{K}^{-1}$) of the porous fin can be obtained from following expression

$$k_{eff} = \phi k_f + (1 - \phi)k_s \tag{4}$$

where k_f and k_s are the thermal conductivities of the fluid and fin material respectively in $\text{W m}^{-1}\text{K}^{-1}$.

The following dimensionless parameters are used

$$(X; \psi; k_R; \theta) = (x/L; t/L; k_s/k_f; (T - T_a)/(T_b - T_a)) \tag{5a}$$

$$\Theta = k_{eff}/k_f = \phi + k_R - \phi k_R \tag{5b}$$

$$[m_1; m_2] = \left[(Ra Da) / (\psi^2 \Theta); \{2Nu(1 - \phi)\} / (\psi^2 \Theta) \right] \tag{5c}$$

$$[Ra; Da; Nu] = \left[\{\rho C_p g \beta (T_b - T_a) t^3\} / (\gamma k_f); K/t^2; ht/k_f \right]. \tag{5d}$$

Using Eqs. (2)-(5), Eq. (1) can be expressed as

$$d^2\theta/dX^2 - m_1\theta^2 - m_2\theta = 0. \tag{6}$$

2.2 Boundary conditions

The boundary conditions in non-dimensional form are

$$\theta = 1 \text{ at } X = 1 \quad (\text{Fin base}) \tag{7a}$$

$$\left[\frac{d\theta}{dX} \right]_{X=0} = H = (Nu/\Theta\psi)\theta_t \quad (\text{Convective tip}) \tag{7b}$$

where $\theta_t = (T_t - T_a)/(T_b - T_a)$ is the dimensionless tip temperature.

2.3 Temperature distribution

The present problem adopts the homotopy perturbation method [19, 20] for obtaining the temperature distribution from the non-linear governing differential equations. According to HPM, the homotopy of Eq. (6) is written as

$$d^2v/dX^2 - d^2\theta_0/dX^2 + p d^2\theta_0/dX^2 + p(-m_1v^2 - m_2v) = 0. \tag{8}$$

The solution of Eq. (8) can be written as

$$v = v_0 + p v_1 + p^2 v_2 + p^3 v_3 + \dots \tag{9}$$

The first approximation is considered as

$$\theta_0 = \theta_t + HX. \tag{10}$$

Substituting Eq. (9) into Eq. (8) and equating the terms with the identical powers of p gives

$$p^0 : d^2v_0/dX^2 - d^2\theta_0/dX^2 = 0 \tag{11}$$

$$p^1 : d^2v_1/dX^2 + d^2\theta_0/dX^2 - m_1v_0^2 - m_2v_0 = 0 \tag{12}$$

$$v_1|_{X=0} = 0, [dv_1/dX]_{X=0} = 0 \tag{13}$$

$$p^2 : d^2v_2/dX^2 - 2m_1v_0v_1 - m_2v_1 = 0 \tag{14}$$

$$v_2|_{X=0} = 0, [dv_2/dX]_{X=0} = 0 \tag{15}$$

$$p^3 : d^2v_3/dX^2 - m_1v_1^2 - 2m_1v_0v_2 - m_2v_2 = 0 \tag{16}$$

$$v_3|_{X=0} = 0, [dv_3/dX]_{X=0} = 0 \tag{17}$$

$\vdots = \vdots$

Solving Eqs. (11)-(17) yields the following

$$v_0 = \theta_i + HX \tag{18}$$

$$v_1 = X^2(m_2\theta_i + m_1\theta_i^2)/2 + X^3(Hm_2 + 2Hm_1\theta_i)/6 + X^4H^2m_1/12 \tag{19}$$

$$v_2 = X^4(m_2^2\theta_i + 3m_1m_2\theta_i^2 + 2m_1^2\theta_i^3)/24 + X^5(10Hm_1^2\theta_i^2 + 10Hm_1m_2\theta_i + Hm_2^2)/120 + X^6(H^2m_1m_2 + 2H^2m_1^2\theta_i)/72 + X^7H^3m_1^2/252 \tag{20}$$

$$v_3 = X^6(11m_1m_2^2\theta_i^2 + m_2^3\theta_i + 20m_1^2m_2\theta_i^3 + 10m_1^3\theta_i^4)/720 + X^7H(m_1m_2^2\theta_i/120 + m_2^3/5040) + X^7Hm_1^2m_2\theta_i^2/42 + X^7Hm_1^3\theta_i^3/63 + 5X^8H^2m_1^2m_2\theta_i/672 + \dots \tag{21}$$

$\vdots = \vdots$

The final temperature distribution in the fin is given as

$$\theta = \lim_{p \rightarrow 1} v = v_0 + v_1 + v_2 + v_3 + \dots \tag{22}$$

2.4 Actual heat transfer rate and fin efficiency

The actual heat transfer rate is calculated by applying Fourier's law of heat conduction at fin base. Actual heat transfer rate (q_a) and ideal heat transfer rate (q_i) in dimensional form are

$$\begin{bmatrix} q_a \\ q_i \end{bmatrix} = \begin{bmatrix} k_{eff}tW[dT/dx]_{x=L} \\ 2hL(t+W)(1-\phi)(T_b - T_a) + \dot{m}C_p(T_b - T_a) + htW(T_b - T_a) \end{bmatrix} \tag{23}$$

where $\dot{m} = \rho V W L$ and $V = gK\beta(T_b - T_a)/\gamma$.

Actual heat transfer rate (Q_a) and ideal heat transfer rate (Q_i) per unit width in dimensionless form are as follows:

$$\begin{bmatrix} Q_a \\ Q_i \end{bmatrix} = \frac{1}{k_f(T_b - T_a)} \begin{bmatrix} q_{act} \\ q_{ideal} \end{bmatrix} = \begin{bmatrix} \Theta\psi[d\theta/dX]_{X=1} \\ \{2Nu(1-\phi)\}/\psi + RaDa/\psi + Nu \end{bmatrix} \tag{24}$$

Thus fin efficiency is given by

$$\eta = Q_a/Q_i \tag{25}$$

3. Optimization analysis

Since transferring heat effectively is the primary function of a fin, so here the aim is to maximize the actual heat transfer rate for a specified fin volume by optimizing four crucial fin parameters which have been selected through significant parameter analysis discussed in subsequent section. In this work the positions of each particle (in PSO) is represented in a four dimensional space by ϕ, ψ, Da and Nu . The objective function of the present work thus can be represented by

$$\text{Maximize } F(Z) = Q_a = \Theta\psi[d\theta/dX]_{X=1} \tag{26}$$

where $Z = [\phi, \psi, Nu, Da]$.

The volume per unit width of a rectangular fin, which is the constraint here, in dimensionless form depends on Nu and ψ which is written as:

$$U = h^2\bar{U}/k_f^2 = Nu^2/\psi \tag{27}$$

The constraints imposed on the variables are:

$$0.4 \leq \phi \leq 0.6; 0.01 \leq \psi \leq 0.10; 10 \leq Nu \leq 50; 0.0001 \leq Da \leq 0.001 \tag{28}$$

4. Particle swarm optimization (PSO)

Inspired by the social behavior of birds, PSO is developed by Kennedy and Eberhart [21], which works quite well in such scenarios which involve nonlinearity as well as noisy fitness landscapes and fetches the near optimum values in less computational effort. It is a non-calculus based optimization technique to solve the global optimization problems. The algorithm starts by creating random particles and assigning random positions to these particles. At every iteration personal previous best or p-best and global best or g-best play a crucial role in improving the particle's positions. The velocity and hence position of each particle is thus updated based on the following equations:

$$v_{i+1} = wv_i + c_1r_1(pbest_i - x_i) + c_2r_2(gbest_i - x_i) \tag{29}$$

$$x_{i+1} = x_i + v_{i+1} \tag{30}$$

The velocity of the particles gets updated as per Eq. (29) while the position gets changed by Eq. (30). Here the acceleration constants c_1 and c_2 are cognitive and social factors respectively which collectively help in changing the velocity during iteration. The random numbers r_1 and r_2 are in the range [0,1]. There are three main parts of Eq. (29) which are the inertia, the cognitive and the social components respectively. A good choice of 'w' which is associated with the momentum of the particles helps to maintain a balance between exploitation and exploration. A modification in original version of PSO considering variable inertia weight instead of a con-

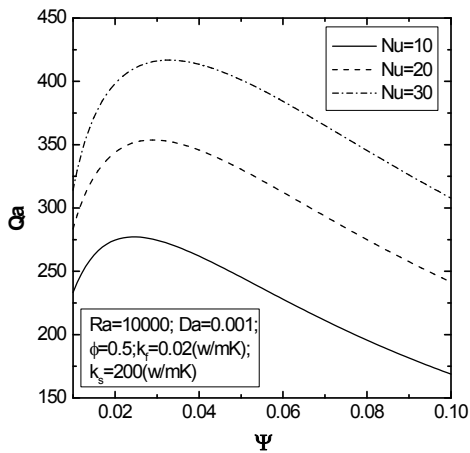


Fig. 2. Significance analysis plot for Q_a vs ψ with variation of Nu .

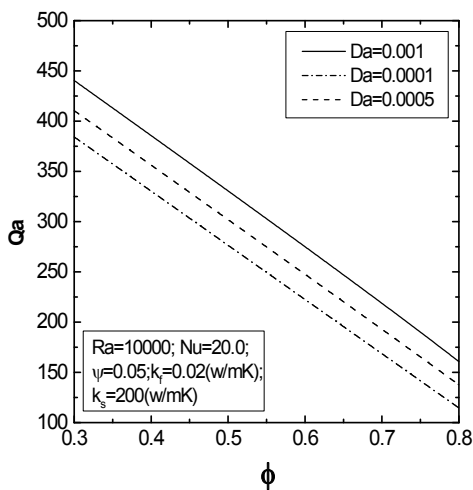


Fig. 3. Significance analysis plot for Q_a vs ϕ with variation of Da .

stant one can yield better results [22]. In this work with the help of reflecting boundary condition [23] the particles are prevented from flying out of the feasible space.

5. Significant variable analysis

A significance analysis has been carried out to gauge the most important or highly sensitive variables out of the seven variables involved in the present problem. This analysis helps to select the most sensitive variables in a problem that influences the output to a greater extent and thus reducing the computational effort and time by omitting the variables which has negligible or insignificant role in the overall output. In the current study the change in heat transfer rate with respect to the change in the values of Ra , Da , Nu , ϕ , T_a , T_b and ψ are noted respectively and based on the gradient the four significant variables (Nu , ψ , ϕ and Da) are selected which has been finally optimized by PSO to achieve greater heat transfer rate by judicious combination of these variables.

Figs. 2 and 3 are generated to show the individual effect of these parameters on heat transfer rate. It is seen from Fig. 2

Table 1. Comparison of temperature distribution between the present analytical and numerical results ($Ra = 10^4$, $Da = 0.0001$, $Nu = 20$, $k_f = 0.02 \text{ Wm}^{-1}\text{K}^{-1}$, $k_s = 200 \text{ Wm}^{-1}\text{K}^{-1}$, $T_b = 373\text{K}$, $T_a = 300\text{K}$, $\phi = 0.4$, $\psi = 0.05$).

X	θ		Difference
	Numerical	HPM	
0.0	0.52307	0.52293	-0.00014
0.2	0.53810	0.53976	0.00166
0.4	0.58854	0.59101	0.00247
0.6	0.67992	0.68090	0.00098
0.8	0.81388	0.81428	0.00040
1.0	1	1	0

that the heat transfer rate enhances with the increase in Nu due to more convection current through the fin surfaces. For each Nu , there is an optimum value of ψ at which the heat transfer rate from the fin attains a maximum value and the optimum value of ψ increases by increasing Nu . Again heat transfer rate is a function of porosity parameter, thermal conductivities, ψ and gradient at the base. With the increase in ψ , gradient is decreased and thus at a particular value of ψ heat transfer becomes maximum. On the other hand, heat transfer rate is decreased by increasing porosity parameter after a certain value. In porous fins, the effective surface area increases, which tends to increase the heat transfer rate, but simultaneously the effective thermal conductivity decreases, which results in decreasing the heat transfer rate. Thus, depending upon the other thermo-physical parameters, the heat transfer rate from the porous fin may becomes less than the solid fin. However, actual heat transfer rate is increased with the increase in Darcy number as seen in Fig. 3. With increasing Da , the fin becomes more permeable which facilitates better flow of fluid through the pores and this enhances the actual heat transfer rate.

6. Results and discussions

The analytical model is validated by comparing the obtained temperature distribution with that obtained from a numerical model, as seen in Table 1. For the numerical result, Eq. (6) is first discretised by central difference scheme of fourth order accuracy followed by solving the difference equations by Gauss Seidel iterative procedure, satisfying the boundary conditions and a convergence criterion of 10^{-6} . As seen in Table 1, the temperature distribution from the present analytical model show a high accuracy with that obtained from the numerical model.

The temperature along the fin length is slightly lower when the value of Darcy number (Da) is higher as seen in Fig. 4. This is because with the increase in Da , the permeability increases which allows more heat to flow out of the fin through the pores thereby reducing the temperature. Again, the temperature along the fin length drops as the porosity of the fin increases. The reason for this trend is two folds. Firstly, at

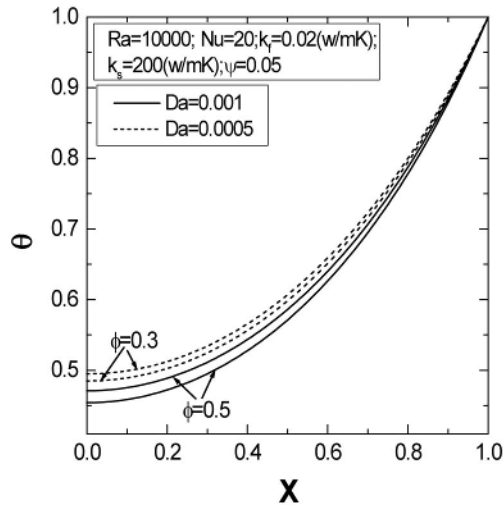


Fig. 4. Temperature distribution with the variation of Da and ϕ .

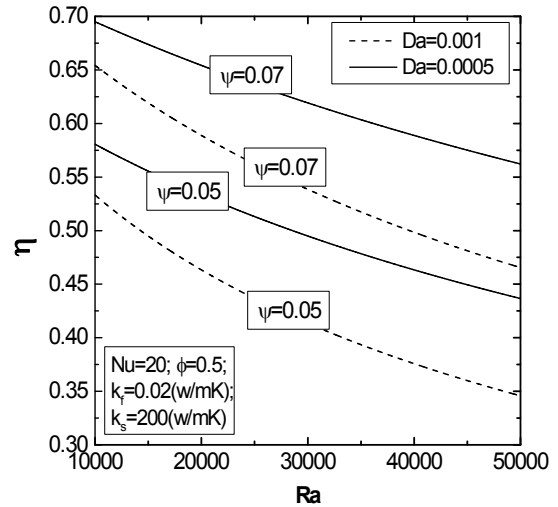


Fig. 6. Efficiency plots as a function of Ra , ψ and Da .

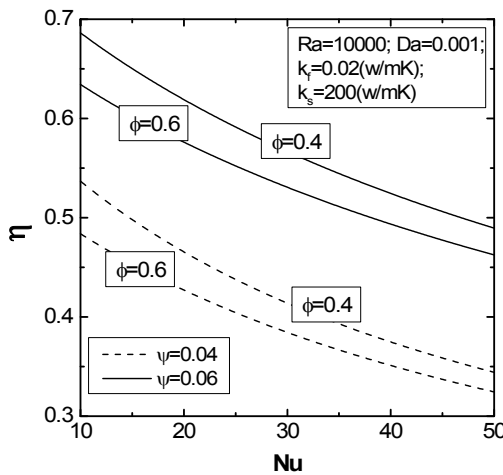


Fig. 5. Efficiency plots as a function of Nu , ψ and ϕ .

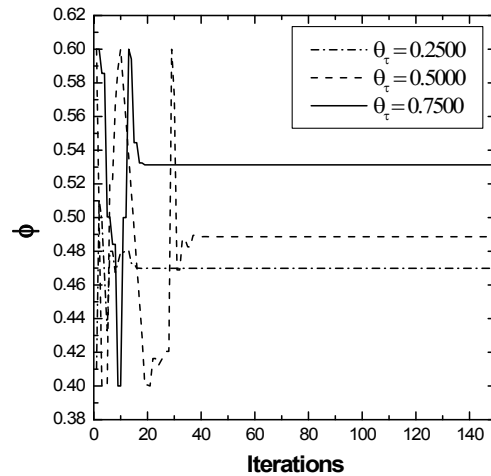


Fig. 7. Convergence plot of significant variable ϕ with three different tip temperatures.

high porosity the effective conductivity suffers due to the removal of excess material and secondly due to higher pore density ambient cool air mixes well with the hot air in fin surface. As seen in Figs. 5 and 6 as ψ increases, fin efficiency increases. It is because at a particular thickness, as the length decreases the conduction resistance reduces. Again, in Fig. 5, it is seen that efficiency decreases with increasing ϕ value. This is because as the pores increases, the heat transfer drops due to the removal of metal which in turn reduces the conductive heat transfer.

Darcy number which is related with permeability improves the efficiency at lower values as seen in Fig. 6. It is because at higher Da the increase in permeability comes at the cost of increase in ideal heat transfer which nullifies the effect of increased value of actual heat transfer to the extent of lowering the efficiency. The same justification can be given for the fall in efficiency in the same figure with increase in Ra values. As the buoyant forces increases, the ideal heat transfer increases at a rate higher than the actual heat transfer. The vari-

ables are varied to understand their importance in temperature distribution and efficiency. This being done, the four important parameters are chosen for optimization to determine a sufficiently good heat transfer rate.

Figs. 7-10 show the convergence plots of four parameters with iteration number. Each parameter is studied for three different fin tip temperatures under consideration. PSO being a metaheuristic technique converges faster to near optimum or good values. It however cannot guarantee the best or optimum results [24] due to randomness present in the algorithm which is an integral identity of metaheuristics. However the aim here is to reach a seemingly good near optimum value. Fig. 7 shows the plot of porosity whose feasible region lies from 0.4 to 0.6. The graph shows fluctuating tendency of the variable in the initial iterations which slowly converges to a good point as shown in figure. Similar trend is seen in the other parameters (ψ and Nu and Da) in Figs. 8-10.

The initial fluctuations seen in all the four variables in three

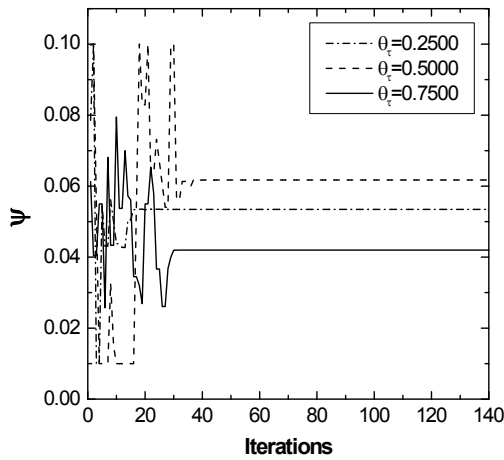


Fig. 8. Convergence plot of ψ with different tip temperatures.

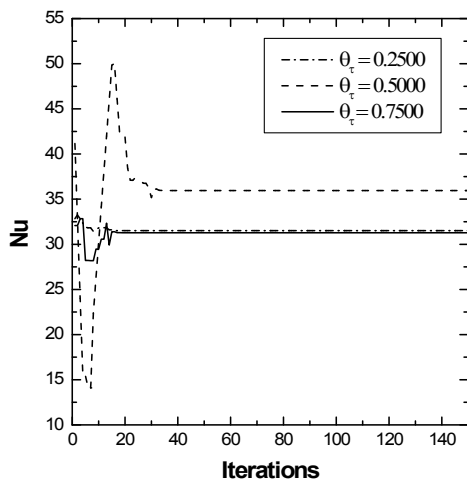


Fig. 9. Convergence plot of Nu with different tip temperatures.

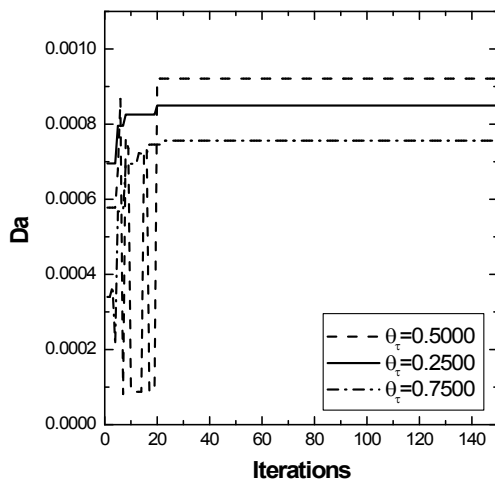


Fig. 10. Convergence plot of Da with different tip temperatures.

different tip temperatures can be understood from PSO’s nature of scanning the domain for the best possible combination of values of the variables that yield the maximum value of

Table 2. Optimized values of the variables obtained from PSO for three different tip temperatures ($Ra = 10^4$, $k_r = 0.02 \text{ Wm}^{-1} \text{ K}^{-1}$, $k_s = 200 \text{ Wm}^{-1} \text{ K}^{-1}$, $T_b = 373 \text{ K}$, $T_a = 300 \text{ K}$).

Tip temperature θ_t	ϕ	ψ	Da	Nu	Q_a (max)
0.25	0.4699	0.05345	0.001	31.5119	1098.591
0.50	0.48861	0.06172	0.001	35.9544	1243.739
0.75	0.53133	0.04949	0.001	31.2791	2697.160

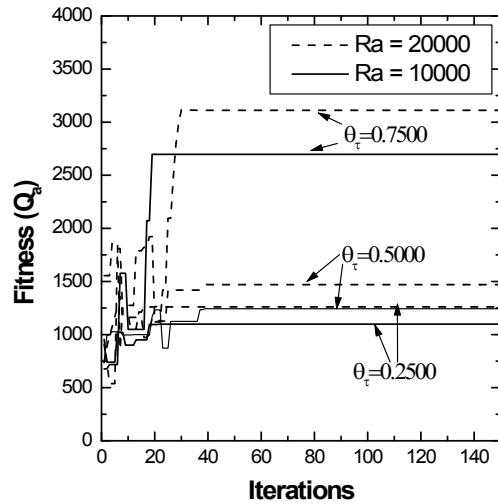


Fig. 11. Convergence pattern of fitness function (heat transfer rate) by varying Rayleigh number with three different tip temperatures.

objective function without disobeying the constraint. Once a good combination is obtained, the variables converge to their individual best or near best values so as to produce an enhanced heat transfer rate. Table 2 shows the optimized values of the variables obtained from PSO for three different tip temperatures.

Rayleigh number plays a crucial role in heat transfer at higher tip temperatures in convective medium. This dimensionless parameter which is associated with buoyant forces, results in better heat transfer through the fin at higher values. This happens because at higher values of Rayleigh number the buoyancy increases which in turn encourages convective heat transfer to take place at a greater scale. The trend obtained from the convergence analysis of the fitness function i.e., actual heat transfer rate is in accordance with the said logic. In Fig. 11, the convergence pattern is studied with respect to the number of iterations for two different Rayleigh number for three tip temperatures. The heat transfer rate increases with increasing tip temperature due to the increasing temperature difference. Also for each tip temperature, the heat transfer rate is more for higher Rayleigh number because of more driving force due to buoyancy effect.

7. Conclusions

A rectangular porous fin is studied analytically (using HPM) to obtain the temperature distribution and efficiency

under convective fin tip conditions. For three different tip temperatures four important variables are optimized by PSO to maximize the actual heat transfer rate. The key findings of this study are summarized as follows:

- Fin tip temperature is decreased with the increase in Da and ϕ .
- Actual heat transfer rate is increased by increasing Nu and Da . However, with the increase in ϕ heat transfer rate decreases due to mainly conduction loss.
- The variables after being optimized by PSO shows increased heat transfer rate for all the three different tip temperatures and the heat transfer rate enhances with the increase in tip temperature.
- The actual heat transfer increases marginally with the increase in Ra for low tip temperatures whereas the change is somewhat appreciable for high tip temperature.

Nomenclature

C_p	: Specific heat of air at constant pressure ($\text{Jkg}^{-1}\text{K}^{-1}$)
g	: Acceleration due to gravity (ms^{-2})
h	: Convective heat transfer coefficient ($\text{W m}^{-2}\text{K}^{-1}$)
k_R	: Thermal conductivity ratio
L	: Fin length (m)
K	: Permeability of porous fin (m^2)
q_{act}	: Actual heat transfer rate per unit width (Wm^{-1})
Q_a	: Dimensionless actual heat transfer rate per unit width
q_{ideal}	: Ideal heat transfer rate per unit width (Wm^{-1})
Ra	: Rayleigh number
T	: Local fin surface temperature ($^{\circ}\text{C}$)
T_a	: Ambient temperature ($^{\circ}\text{C}$)
T_b	: Fin base temperature ($^{\circ}\text{C}$)
T_t	: Fin tip temperature ($^{\circ}\text{C}$)
\bar{U}	: Fin volume per unit width (m^2)
U	: Dimensionless fin volume per unit width
x	: Axial length measured from fin tip (m)
X	: Dimensionless distance, x/L

Greek symbols

ϕ	: Porosity
β	: Coefficient of thermal expansion (K^{-1})
γ	: Kinematic viscosity (m^2s^{-1})
ψ	: Thickness to length ratio
η	: Fin efficiency
θ	: Dimensionless temperature, $(T-T_a)/(T_b-T_a)$

References

- [1] S. Kiwan, Thermal analysis of natural convection porous fins, *Transport in Porous Media*, 67 (2007) 17-29, Doi: 10.1007/s11242-006-0010-3.
- [2] S. Kiwan, Effect of radiative losses on the heat transfer from porous fins, *Int. J. Therm. Sci.*, 46 (2007) 1046-1055, Doi: 10.1016/j.ijthermalsci.2006.11.013.
- [3] A. Moradi, T. Hayat and A. Alsaedi, Convection-radiation thermal analysis of triangular porous fins with temperature-dependent thermal conductivity by DTM, *Energy Convers. Manage.*, 77 (2014) 70-77, Doi: 10.1016/j.enconman.2013.09.016.
- [4] M. Hatami, A. Hasanpour and D. D. Ganji, Heat transfer study through porous fins (Si_3N_4 and AL) with temperature-dependent heat generation, *Energy Convers. Manage.*, 74 (2013) 9-16, Doi: 10.1016/j.enconman.2013.04.034.
- [5] D. Bhanja and B. Kundu, Thermal analysis of a constructal T-shaped porous fin with radiation effects, *Int. J. Refrig.*, 34 (2011) 1483-1496, Doi: 10.1016/j.ijrefrig.2011.04.003.
- [6] B. Kundu, D. Bhanja and K. S. Lee, A model on the basis of analytics for computing maximum heat transfer in porous fins, *Int. J. Heat Mass Trans.*, 55 (2012) 7611-7622, Doi: 10.1016/j.ijheatmasstransfer.2012.07.069.
- [7] D. Bhanja, B. Kundu and P. K. Mandal, Thermal analysis of porous pin fin used for electronic cooling, *Procedia Eng.*, 64 (2013) 956-965, Doi: 10.1016/j.proeng.2013.09.172.
- [8] D. Bhanja, B. Kundu and A. Aziz, Enhancement of heat transfer from a continuously moving porous fin exposed in convective-radiative environment, *Energy Convers. Manage.*, 88 (2014) 842-853, Doi: 10.1016/j.enconman.2014.09.016.
- [9] S. A. Hazarika, T. Deshamukhya, D. Bhanja and S. Nath, Thermal analysis of a constructal T-shaped porous fin with simultaneous heat and mass transfer, *Chinese J. Chemical Eng.*, 25 (2017) 1121-1136, Doi: 10.1016/j.cjche.2017.03.034.
- [10] B. Kundu and D. Bhanja, An Analytical prediction for performance and optimum design analysis of porous fins, *Int. J. Refrig.*, 34 (2011) 337-352. Doi: 10.1016/j.ijrefrig.2010.06.011.
- [11] R. Das, Forward and inverse solutions of a conductive, convective and radiative cylindrical porous fin, *Energy Convers. Manage.*, 87 (2014) 96-106, Doi: 10.1016/j.enconman.2014.06.096.
- [12] H. S. Kang, Optimization of a rectangular profile annular fin based on fixed fin height, *J. Mech. Sci. Tech.*, 23 (2009) 3124-3131, Doi: 10.1007/s12206-009-0905-3.
- [13] A. Shadlaghani, M. R. Tavakoli, M. Farzaneh and M. R. Salimpour, Optimization of triangular fins with/without longitudinal perforate for thermal performance enhancement, *J. Mech. Sci. Tech.*, 30 (4) (2016) 1903-1910, Doi: 10.1007/s12206-016-0349-5.
- [14] S. A. Hazarika, D. Bhanja, S. Nath and B. Kundu, Thermal design parameters of a wet T-shaped fin for linear variation of humidity ratio with saturation temperature, *J. Mech. Sci. Tech.*, 32 (5) (2018) 2391-2397, Doi: 10.1007/s12206-018-0451-y.
- [15] F. Miao, H. S. Park, C. Kim and S. Ahn, Swarm intelligence based on modified PSO algorithm for the optimization of axial-flow pump impeller, *J. Mech. Sci. Tech.*, 29 (11) (2015) 4867-4876, Doi: 10.1007/s12206-015-1034-9.
- [16] D. B. Kwak, H. P. Kwak, J. H. Noh and S. J. Yook, Optimi-

zation of the radial heat sink with a concentric cylinder and triangular fins installed on a circular base, *J. Mech. Sci. Tech.*, 32 (1) (2018) 505-512, Doi: 10.1007/s12206-017-1252-4.

- [17] V. K. Patel and R. V. Rao, Design optimization of shell-and-tube heat exchanger using particle swarm optimization technique, *Appl. Therm. Eng.*, 30 (2010) 1417-1425, Doi: 10.1016/j.applthermaleng.2010.03.001.
- [18] R. V. Rao and V. K. Patel, Thermodynamic optimization of cross flow plate-fin heat exchanger using a particle swarm optimization algorithm, *Int. J. Therm. Sci.*, 49 (9) (2010) 1712-1721, Doi: 10.1016/j.ijthermalsci.2010.04.001.
- [19] J. He, Homotopy perturbation method: A new nonlinear analytical technique, *Appl. Math. Comput.*, 135 (1) (2003) 73-79, Doi: 10.1016/S0096-3003(01)00312-5.
- [20] E. Cuce and P. M. Cuce, A successful application of homotopy perturbation method for efficiency and effectiveness assessment of longitudinal porous fins, *Energy Convers. Manage.*, 93 (2015) 92-99, Doi: 10.1016/j.enconman.2015.01.003.
- [21] J. Kennedy and R. Eberhart, Particle swarm optimization, *Int. Conf. Neural Networks*, Perth, Australia (1995) 1942-1948, Doi: 10.1109/ICNN.1995.488968.
- [22] M. A. Arasomwan and A. O. Adewumi, On the performance of linear decreasing inertia weight particle swarm optimization for global optimization, *The Scientific World J.* (2013) 1-12, Doi: 10.1155/2013/860289.
- [23] S. Xu and Y. Rahmat-Samii, Boundary conditions in particle swarm optimization revisited, *IEEE Trans. Antennas and Propagation*, 55 (2007) 760-765, Doi: 10.1109/TAP.2007.891562.
- [24] X. S. Yang, Cuckoo search and firefly algorithm: Overview and analysis, *Studies in Comp. Intelligence*, 516 (2013) 1-26, Doi: 10.1007/978-3-319-02141-6_1.



Tuhin Deshamukhya received B.E. in the year 2010 from Sathyabama University and M. Tech in the year 2012 from the National Institute of Technology, Silchar. Currently he is a research scholar in NIT Silchar and his research area includes Application of metaheuristic optimization in porous fins.



Dipankar Bhanja is an Assistant Professor in the Department of Mechanical Engineering in National Institute of Technology Silchar, Assam. His research areas are CFD, Heat Transfer, Constructal theory, Solar energy, Optimization etc. He is the author of more than 20 technical papers published in referred international journals. He is a reviewer of more than 16 International Journals of repute.



Sujit Nath received his Ph.D. degree from Jadavpur University, Kolkata, India. Presently he is an Assistant Professor in the Department of Mechanical Engineering, National Institute of Technology Silchar, Assam, India. His research areas are CFD, Heat Transfer, Atomization, Solar energy, Optimization etc. He is a reviewer in many international journals of repute and also published many technical papers in referred International journals.



Saheera Azmi Hazarika graduated in Mechanical Engineering from Assam Engineering College, Assam, India. She obtained her M. Tech. in Thermal Engineering from National Institute of Technology Silchar, India. Presently she is a research scholar in the Department of Mechanical Engineering, National Institute of Technology Silchar, Assam, India. Her research areas are simultaneous heat and mass transfer, Constructal theory and optimization.